



Design, synthesis and biological evaluation of N^1 -(isoquinolin-5-yl)- N^2 -phenylpyrrolidine-1,2-dicarboxamide derivatives as potent TRPV1 antagonists

Mingxiang Gao^a, Cunbin Nie^a, Jinyu Li^a, Beibei Song^a, Xinru Cheng^a, Erying Sun^a, Lin Yan^{a,*}, Hai Qian^{b,*}

^a Institute for Innovative Drug Design and Evaluation, School of Pharmacy, Henan University, N. Jinming Ave., Kaifeng, Henan 475004, China

^b State Key Laboratory of Natural Medicines, Center of Drug Discovery, China Pharmaceutical University, 24 Tongjiaxiang, Nanjing, Jiangsu 210009, China

ARTICLE INFO

Keywords:

Analgesic
Transient receptor potential vanilloid type 1
5-Aminoisoquinoline urea
Hyperthermia

ABSTRACT

Reported herein is the design, synthesis, and pharmacologic evaluation of a class of TRPV1 antagonists constructed on a N^1 -(isoquinolin-5-yl)- N^2 -phenylpyrrolidine-1,2-dicarboxamide platform that evolved from a 5-aminoisoquinoline urea lead. Advancing the SAR of this series led to the eventual identification of **3b**, comprising a *p*-Br substituted phenyl. In a TRPV1 functional assay, using cells expressing recombinant human TRPV1 channels, **3b** displayed potent antagonism activated by capsaicin ($IC_{50} = 0.084 \mu M$) and protons ($IC_{50} = 0.313 \mu M$). In the preliminary analgesic and body temperature tests, **3b** exhibited good efficacy in capsaicin-induced and heat-induced pain models and without hyperthermia side-effect. On the basis of its superior profiles, **3b** could be considered as the lead candidate for the further development of antinociceptive drugs.

1. Introduction

Transient receptor potential vanilloid 1 (TRPV1) is an ion channel expressed on sensory neurons triggering an influx of cations, which is selectively activated by a wide range of stimuli such as exogenous ligands (e.g., capsaicin or resiniferatoxin), heat ($> 43^\circ C$), acid ($pH < 6.8$), and endogenous substances (e.g., anandamide and oxidative metabolites of linoleic acid) [1–4]. Activation of this channel is associated to chronic inflammatory pain and peripheral neuropathy [5]. Therefore, inhibition of TRPV1 function represents a strategy for the treatment of a variety of disease states, particularly in the management of chronic intractable pain [6,7]. Over the past decade, a number of potent and selective small molecule TRPV1 antagonists has confirmed that pharmacological blockade of this receptor provided analgesic efficacy in several models of inflammatory and neuropathic pain [8–10]. However, the tendency of some TRPV1 antagonists to induce hyperthermia side-effect in preclinical models turned out to be a hurdle and led to its withdrawal from clinical development [11]. As a result, pharmacological separation of analgesic and hyperthermic effects became the key challenge in developing TRPV1 antagonists as therapeutic agents for pain management. Recently, efforts to eliminate hyperthermia led to the identification of the relative responses of

TRPV1 to various stimulatory modulators, where whether TRPV1 antagonists block responses both to capsaicin and low pH or whether they selectively antagonize capsaicin only [12,13]. Reported herein is the design, synthesis and evaluate for their activity of TRPV1 antagonists constructed on a 5-aminoisoquinoline urea fragment (Fig. 1). The early lead compound **1** which belonged to the “first-generation” TRPV1 antagonists exhibited good potency at the target, modest efficacy in animal pain models, and less than desirable pharmacokinetic profile [14,15]. It bears emphasizing, that most of the “first-generation” antagonists block, in a dose-dependent manner, all modes of TRPV1 activation (capsaicin, endogenous lipids, acidic pH, heat) can elicit hyperthermia [16]. More recently, the isoquinoline urea derivative **2** which including chromane moiety and with *R* configuration was found to be a modality-differentiated second-generation TRPV1 antagonist with good analgesic efficacy and a temperature-neutral profile [9]. In contrast to first-generation antagonists that inhibit all modes of TRPV1 activation and can elicit hyperthermia, compound **2** fully block TRPV1 activation by capsaicin but only partially block TRPV1 activation by acid and devoid of hyperthermic effects at high dose. These data encouraged a more focused investigation of SAR to optimization of the isoquinoline urea series TRPV1 antagonists. In this study, to look for another class of potent TRPV1 antagonists and further explore the

* Corresponding authors.

E-mail addresses: yanlin0378@163.com (L. Yan), qianhai24@163.com (H. Qian).

<https://doi.org/10.1016/j.bioorg.2018.09.033>

Received 5 July 2018; Received in revised form 22 September 2018; Accepted 24 September 2018

Available online 25 September 2018

0045-2068/ © 2018 Elsevier Inc. All rights reserved.

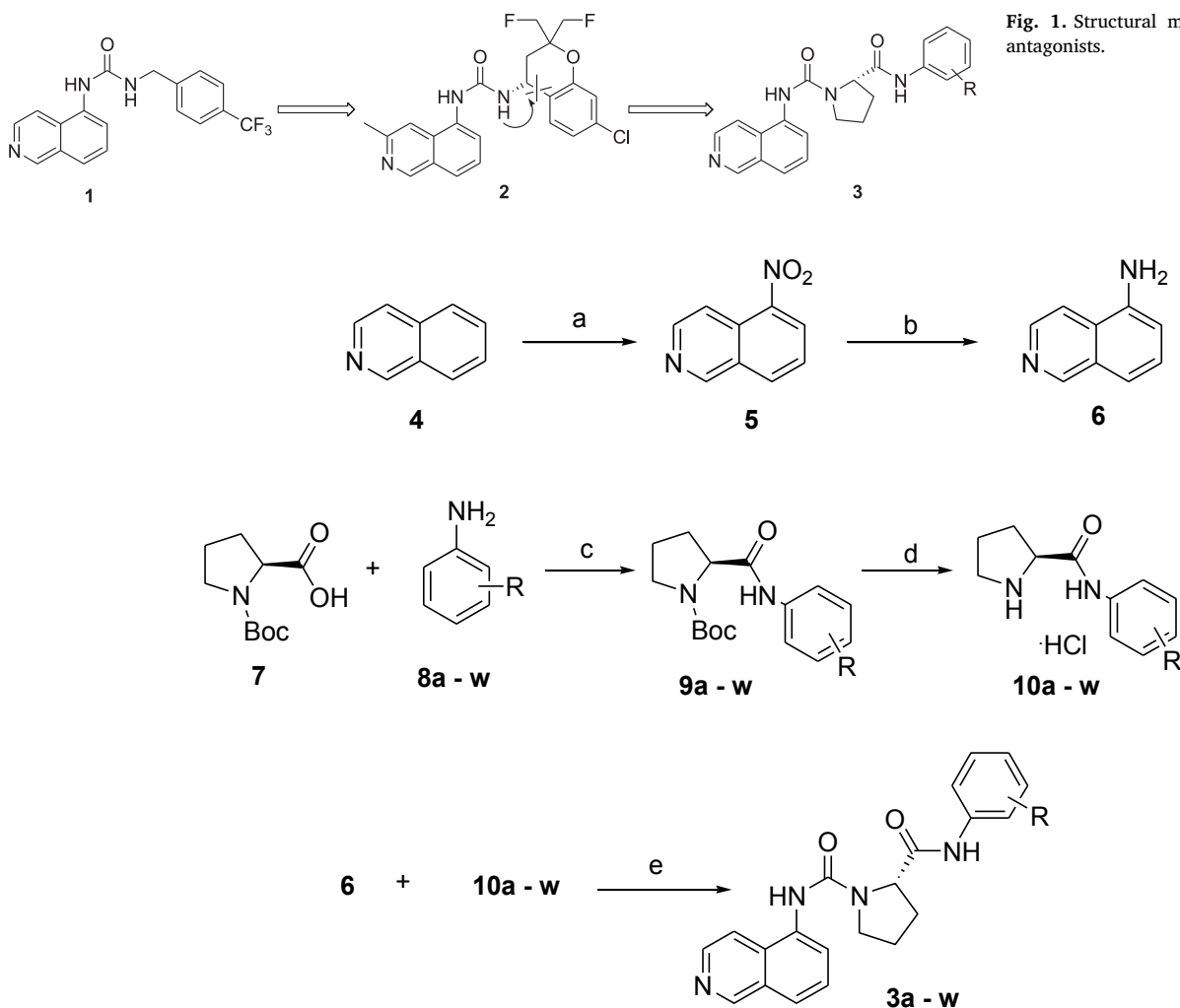


Fig. 1. Structural modifications of TRPV1 antagonists.

Scheme 1. Synthesis of the target compounds 3. Reagents and conditions: (a) HNO_3 , H_2SO_4 , -15°C ; (b) Pd/C, CH_3OH , rt; (c) EDCl/DMAP; (d) HCl/EtOAc; (e) triphosgene/DMAP, CH_2Cl_2 , one pot.

isoquinoline urea, the pyrrolidine ring was designed to maintain the distance and constrained nature of the phenyl ring, whereas the chromane ring was cleaved, leading to compound **3b**, a novel TRPV1 antagonist with good analgesic efficacy and a temperature-neutral profile (Fig. 1).

2. Results and discussion

2.1. Chemistry

The synthesis of the target compounds **3** were accomplished by urea coupling between the two corresponding amines (**6**, **10**) as described in Scheme 1. Intermediate **6** was prepared via nitration of commercially available isoquinoline (**4**) and subsequent reduction using Pd/C as a catalyst. The synthesis of another intermediate (**10**) was accomplished starting from *N*-Boc-L-proline (**7**). Reaction of compound **7** with substituted anilines produced pyrrolidine carboxamides **9a-w**. The Boc protecting group was removed under acidic conditions (HCl), leading to **10a-w** in high yield for coupling. The coupling between **6** and **10a-w** in the presence of triphosgene provided the target compounds **3a-w**. The structures of all target compounds are presented in Table 1.

2.2. Structure–activity relationship (SAR) analysis

Firstly, all of the new compounds were evaluated for their ability to

block capsaicin (CAP) or low pH-induced activation of human TRPV1 channels. The results are presented in Table 1, together with the potency of the classical TRPV1 antagonist BCTC (*N*-(4-(tert-butyl)phenyl)-4-(3-chloropyridin-2-yl)piperazine-1-carboxamide). A variety of substituents such as the small lipophilic halogen group, bulky tert-butyl group, even the multisubstituted benzene rings were basically well tolerated. The effects of changing the position of the substituent were also investigated. In CAP assay, the *para*-substitution was superior to *meta*-substitution or *ortho*-substitution. The representative examples include phenyls with bromine (**3b** vs **3c**, **3d**), chlorine (**3g** vs **3e**, **3f**), methoxyl (**3i** vs **3h**), and methyl (**3j** vs **3k**) substitutions (Table 1). However, in pH assay, these *para*-substitution compounds showed dramatic decrease in potency than substitutions at *meta*- and *ortho*-positions, while that of **3i**, resulted in a minor increase in activity (compare **3i** $\text{IC}_{50} = 0.049 \mu\text{M}$ vs **3h** $\text{IC}_{50} = 0.054 \mu\text{M}$).

Next, to develop more efficient analgesic candidates with minimized side-effects, all of the new compounds were advanced into our preliminary *in vivo* analgesic studies and side-effects tests. Initially, when administered orally in mice, most of compounds were found to be nearly not efficacious at 1 and 10 mg/kg, in comparison with vehicle group (data not shown). We subsequently examined the analgesic activities using the dose of 30 mg/kg. The analgesic activity *in vivo* of each compounds were evaluated by three different models of pain (Fig. 2). In the capsaicin test, the total time spent licking the paw was significantly reduced by all test compounds compared to the vehicle (Fig. 2A). In

Table 1
In vitro ability of compounds to inhibit the activation of hTRPV1 receptors.

Compounds	R	hTRPV1(CAP) IC ₅₀ ^a (μM)	hTRPV1(pH) IC ₅₀ ^b (μM)
3a	H	0.481 ± 0.072	0.038 ± 0.015
3b	4-Br	0.084 ± 0.019	0.313 ± 0.023
3c	3-Br	0.239 ± 0.087	0.059 ± 0.042
3d	2-Br	0.216 ± 0.102	0.064 ± 0.017
3e	2-Cl	ND	0.041 ± 0.036
3f	3-Cl	3.1 ± 0.1	0.056 ± 0.049
3g	4-Cl	0.416 ± 0.064	0.128 ± 0.092
3h	2-OCH ₃	0.451 ± 0.087	0.054 ± 0.043
3i	4-OCH ₃	0.195 ± 0.041	0.049 ± 0.047
3j	4-CH ₃	0.314 ± 0.094	0.307 ± 0.124
3k	3-CH ₃	0.382 ± 0.029	0.046 ± 0.075
3l	3- <i>i</i> Pr	ND	0.035 ± 0.014
3m	4- <i>t</i> Bu	0.211 ± 0.031	0.135 ± 0.062
3n	4-F	0.199 ± 0.053	0.171 ± 0.078
3o	2-CH ₃ , 4-OCH ₃	0.208 ± 0.047	0.214 ± 0.056
3p	2-Cl, 4-Br	ND	ND
3q	3-Cl, 4-CH ₃	0.234 ± 0.071	0.011 ± 0.025
3r	2, 6-di-CH ₃	ND	0.0067 ± 0.0097
3s	2, 4-di-CH ₃	0.497 ± 0.068	ND
3t	3-Cl, 4-OCH ₃	2.8 ± 0.2	ND
3u	3, 4-di-Cl	0.204 ± 0.062	0.0056 ± 0.0042
3v	3, 5-di-OCH ₃	1.9 ± 0.3	ND
3w	2, 4, 6-tri-CH ₃	0.412 ± 0.082	0.0089 ± 0.0059
BCTC		0.017 ± 0.045	0.0032 ± 0.0098

ND, not determined.

^a Human TRPV1 receptor activated by capsaicin.

^b Human TRPV1 receptor activated by low pH (5.0). Unless otherwise stated, all values are the mean (SEM of at least three separate experiments).

In addition, most of the test compounds were superior to positive control BCTC, especially **3b**, **3i**, **3n**, **3o** and **3u** exhibited greater potency than BCTC. Once more, the *para*-substitution was the favorable site for higher potency. For instance, *p*-Br substituted **3b** was more potent than *m*-Br substituted **3c** or *o*-Br substituted **3d**. In the abdominal constriction test, all compounds reduced the number of writhes in proto-induced pain models and many test compounds exhibited better potency than BCTC (Fig. 2B). Of particular interest was the compound **3b** which was the most active compound in the capsaicin test, had much weaker effect compared to other compounds, but consistent with the activity observed in pH assay. In the tail-flick test, a variety of substituents are well tolerated (Fig. 2C). Evidently, better %MPE in treatment of heat-induced pain were obtained from *para*-substitution compounds such as **3b**, **3g**, **3j** and **3n**. Overall, all the test compounds had antinociceptive activity to a certain extent. Basically all of the compounds were efficacious in capsaicin-induced pain and in the tail-flick test, but some of test compounds such as **3b**, **3j** and **3n** lacked efficacy in the abdominal constriction test. To our delight, recent reports have indicated that the hyperthermic effect of a TRPV1 antagonist is related to the extent to which it causes blockade in proton mode. Indeed, some TRPV1 antagonists which only minimally blocking acid activation of TRPV1, have been identified do not elevate core body temperature in pre-clinical models [9].

In a follow-up experiment, potent compounds (i.e., those exhibiting acceptable *in vivo* and *in vitro* potency) were further assessed for their body temperature and compared their effects with positive control BCTC (Fig. 3). A single oral dose of 30 mg/kg was administered to mice, and core body temperature was evaluated over 2 h using a rectal thermometer. In our tests, there were significant increases by almost all test compounds on body temperature beginning 30 min after administration and lasting for at least 90 min, and with a maximum of Δtemperature occurring at 60 min. In contrast, compound **3b** which exhibited very weak effect in low pH-induced activation of human TRPV1 channel test, did not exhibit significant effects relative to vehicle. Furthermore, as previously mentioned in the three analgesic tests, **3b** was effective in treatment of capsaicin-induced and heat-induced

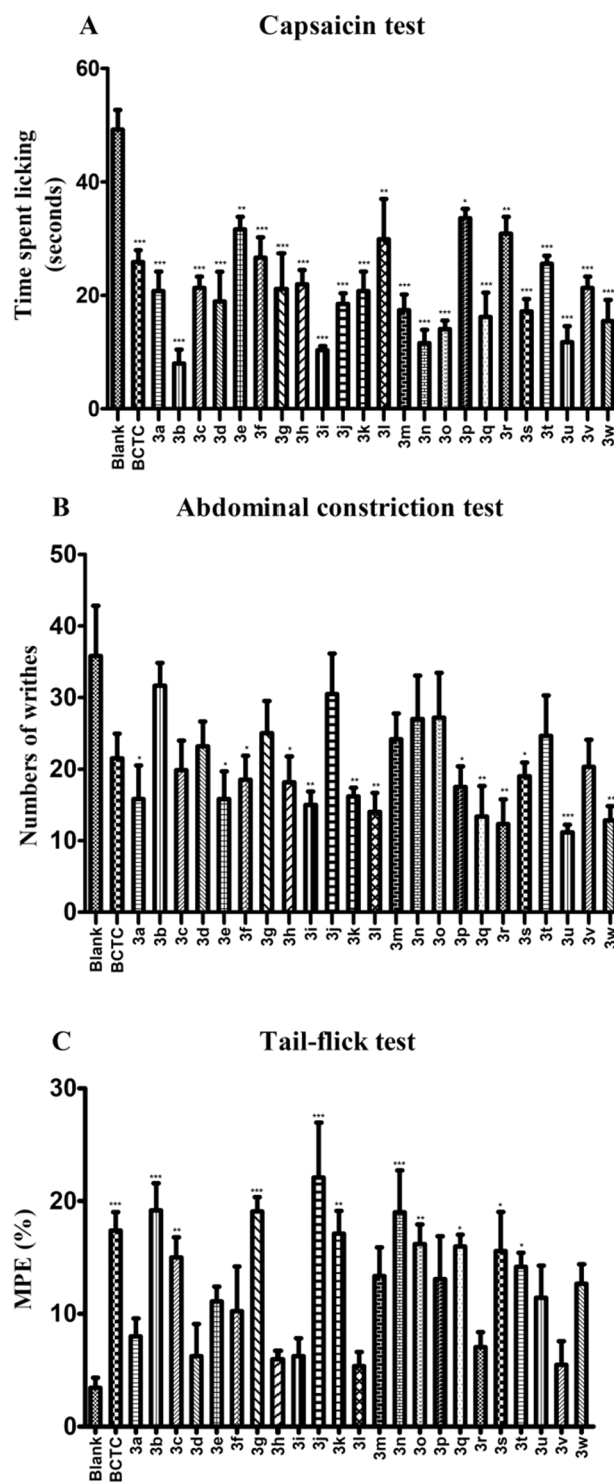


Fig. 2. Analgesic activities of synthesized compounds in 30 mg/kg after oral administration. (A) The antinociceptive effects in the capsaicin test; (B) suppression of acetic acid-induced writhing response; (C) inhibition of thermal nociception by synthesized compounds. Each bar represents the mean ± SEM (n = 8). Statistical analysis was evaluated using a one-way analysis of variance (ANOVA) followed by Dunnett's multiple comparison test. *p < 0.05; **p < 0.01; ***p < 0.001 compared with the vehicle group.

pain, and not effective in proton-induced pain. Compared to **3b**, compounds **3q** and **3u** exhibited good analgesic potencies in acid-induced, capsaicin-induced pain and caused hyperthermia in mice. Of the compounds evaluated *in vitro* TRPV1 antagonistic activity, *in vivo* model of pain and body temperature, **3b** emerged as a preferred compound and

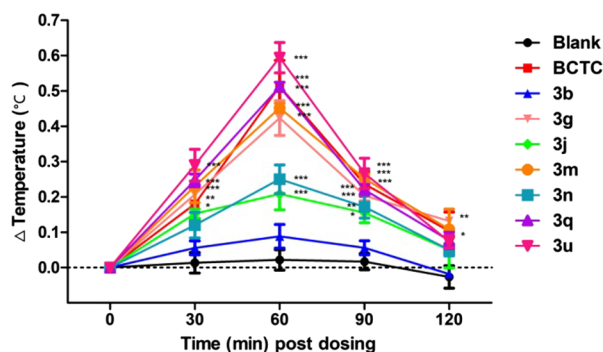


Fig. 3. The effects of compounds in 30 mg/kg after oral administration on body temperature in mice. The changes of body temperature after dose. Data are expressed as mean \pm SEM (n = 8). *p < 0.05, **p < 0.01; ***p < 0.001 by Dunnett's multiple comparison test compared with the vehicle-treated group.

exhibited superior pharmacodynamic properties. Therefore, it was evaluated in more detail.

Focusing in particular on dose-response analyses to better determine the efficacy of **3b**, some additional experiments had been carried out. First, analgesic activities of compound **3b** at different doses were assessed (Fig. 4). In the capsaicin-induced pain model study, **3b** (i.g., 30 min before capsaicin) dose-dependently reduced the total time spent licking the paw (Fig. 4A). In addition, the oral administration of 10 mg/kg and 60 mg/kg of **3b** were similar to an oral dose of 30 mg/kg of **3b**, which exhibited greater potency than BCTC. In the abdominal constriction test, though pretreatment with **3b** (i.g., 30 min before the injection of acetic acid) dose-dependently reduced the number of writhes the effect was not significant and much weaker than BCTC (30 mg/kg i.g.) did (Fig. 4B). Similarly, in the tail-flick test compound **3b**-produced antinociception was dose-dependent (Fig. 4C). Compound **3b** (1 mg/kg) had a similar %MPE to the vehicle group, while **3b** (30 mg/kg) and **3b** (60 mg/kg) showed higher %MPE than BCTC (30 mg/kg). From the above analgesic activity tests, the compound **3b** exhibited good analgesic potency in capsaicin-induced and heat-induced pain models and the antinociception effect was dose-dependent. However, the analgesic activity tests also indicated that the compound **3b** exhibited differentiated effects on capsaicin-induced and acetic acid-induced pain model.

To explore this further with the compound **3b**, the dose-response studies were administered to mice, and core body temperature was evaluated over 2 h using a rectal thermometer. As illustrated in Fig. 5, no significant changes in core body temperature were observed in all the doses of **3b** versus vehicle when monitored over a period of 2 h. While a 30 mg/kg po dose of BCTC significantly increased temperature

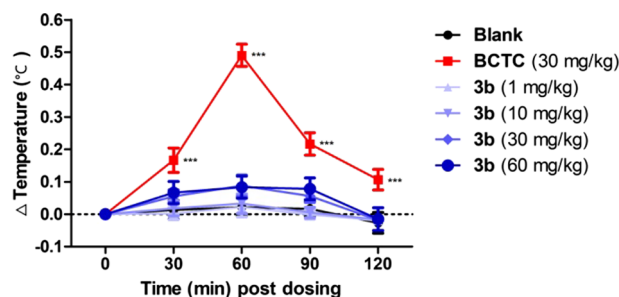


Fig. 5. The effects of compound **3b** at different doses on body temperature in mice. The changes of body temperature after dose. Data are expressed as mean \pm SEM (n = 8). *p < 0.05, **p < 0.01; ***p < 0.001 by Dunnett's multiple comparison test compared with the vehicle-treated group.

relative to vehicle, beginning 30 min after administration and lasting for at least 2 h. In general, the analgesic activity of **3b** was in a dose-dependent manner and over all times and doses of **3b**, the average change of core body temperature was not significantly above vehicle.

On the basis of its potent *in vitro* activity at hTRPV1, good analgesic activity in capsaicin-induced and heat-induced pain models and without hyperthermia side-effect, compound **3b** was selected for further study. The results of both the *in vitro* TRPV1 activities in rat and the pharmacokinetic profiles were reported in Table 2. Results from *in vitro* rTRPV1 antagonistic activities showed that compound **3b** was also potent antagonist against rat TRPV1 (rTRPV1). Consistent with its *in vitro* hTRPV1 antagonistic activities, **3b** exhibited poor antagonism toward pH. In addition, high aqueous solubility is widely recognized as a requirement for good *in vivo* bioavailability. According to the Log P values (the calculated octanol-water partition coefficient), compound **3b** was less lipophilic (logP 2.56) than compound **1** (logP 3.16) and **2** (logP 3.46). Of course, one concern is that predicted Log P values have significant uncertainty. We subsequently identified compound **3b** showed satisfactory aqueous solubility (> 100 μ M). The pharmacokinetic parameters of **3b** administered in oral were also summarized in Table 2. As shown in Table 2, compound **3b** exhibited moderate C_{max} (119.3 \pm 35.1 ng/mL), and modest half-life (1.4 \pm 0.3 h) as well as relatively moderate bioavailability (F = 23%) in rats after oral administration of 30 mg/kg.

3. Conclusions

In conclusion, this work summarizes the transformation of an early 5-aminoisoquinoline urea motif into a N¹-(isoquinolin-5-yl)-N²-phenylpyrrolidine-1,2-dicarboxamide-based design and its optimization to produce **3b**. Close scrutiny of our pharmacology data revealed **3b** was a

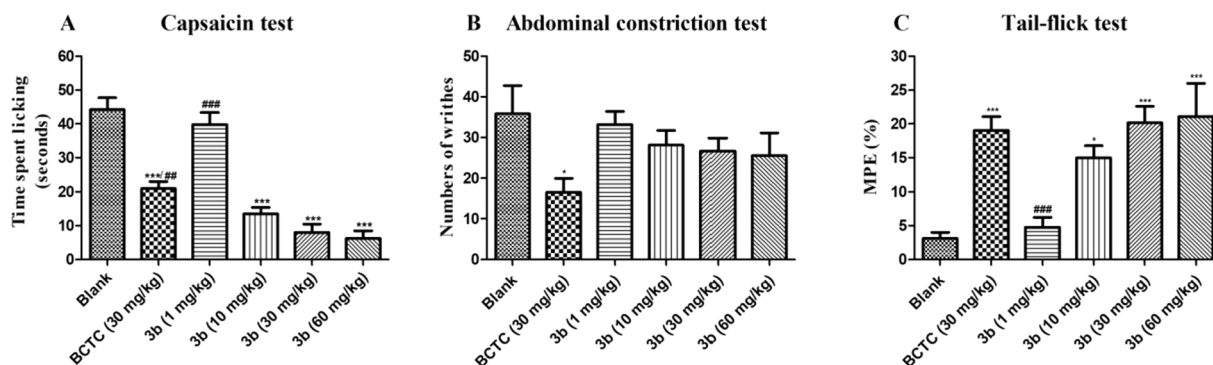


Fig. 4. Analgesic activities of compound **3b** at different doses. (A) The antinociceptive effects in the capsaicin test; (B) suppression of acetic acid-induced writhing response; (C) inhibition of thermal nociception. Each bar represents the mean \pm SEM (n = 8). Statistical analysis was evaluated using a one-way analysis of variance (ANOVA) followed by Dunnett's multiple comparison test. *p < 0.05; **p < 0.01; ***p < 0.001 compared with the vehicle group; #p < 0.05; ##p < 0.01; ###p < 0.001 compared with the **3b** (30 mg/kg) group.

Table 2
In vitro TRPV1 activities and the pharmacokinetic profile^d of compound **3b**.

Characteristic	3b
rTRPV1(CAP) IC ₅₀ ^a (μM)	0.1543 ± 0.058
rTRPV1(pH) IC ₅₀ ^b (μM)	0.6984 ± 0.187
Log P ^c	2.56
Solubility pH 6.8 (μM)	> 100
t _{1/2} (h)	1.4 ± 0.3
Cmax (ng/mL)	119.3 ± 35.1
bioavailability, Foral (%)	23

^a Rat TRPV1 receptor activated by capsaicin.

^b Rat TRPV1 receptor activated by low pH (5.0). Unless otherwise stated, all values are the mean (SEM of at least three separate experiments).

^c Log P values calculated by ChemDraw.

^d Pharmacokinetic analysis determined in rat (three animals per group each oral) following administration of 30 mg/kg.

potent TRPV1 antagonist that exhibited excellent *in vitro* functional activity and good efficacy in capsaicin-induced and heat-induced pain models. Further experiments showed that the antinociception effects produced by **3b** were dose-dependent and the analgesic mechanism of **3b** may be mainly by blocking heat-induced and capsaicin-induced TRPV1 activation without hyperthermia. In addition, compound **3b** displayed promising pharmacokinetic properties in rats following oral administration. Taken together, this investigation has provided us with novel scaffolds for the further study of related TRPV1 antagonists.

4. Experimental

4.1. Biological methods

The synthesized compounds were investigated for TRPV1 antagonistic *in vitro*, *in vivo* analgesic activity and the effect on body temperature. The test compounds and the standard drugs were administered in the form of a suspension (using 0.5% sodium carboxymethyl cellulose as a vehicle) by intragastric administration. Separate groups of KM male mice ($n = 8$), weighing 18–22 g, were pretreated with compounds (30 mg/kg unless otherwise indicated) 30 min before the test. The animals were procured from the Comparative Medicine Centre of Yangzhou University (Jiangsu, China) and were maintained in colony cages at 25 ± 2 °C, relative humidity 45–55%, under a 12 h light/dark cycle; they were fed standard animal feed. All the animals were acclimatized for a week before use. The Institutional Animal Ethics committee has approved the protocol adopted for the experimentation of animals.

4.1.1. Transient receptor potential vanilloid type1 antagonistic activity assays *in vitro*

Culture plates with Ca²⁺- and Mg²⁺-free phosphate-buffered saline supplemented with 5 mM ethylenediaminetetra-acetic acid were used for the TRPV1 aequorin cells (Perkin Elmer, Waltham, MA, USA) growth. The cells were pelleted for 2 min at 1000g; resuspended in Dulbecco's minimum essentialmedium-F12 medium with 15 mM HEPES (pH 7.0) and 0.1% BSA (assay buffer) at a density of 3 × 10⁵ cells/mL and incubated for 4 h in the dark in the presence of 5 mM Coelenterazine (Promega, Madison, WI, USA). After loading, cells were diluted with assay buffer to a concentration of 5 × 10⁶ cells/mL. Twenty microliter of cells was injected over 20 μL of the sample solution plated on 384-well plates, respectively, unless otherwise indicated. The Digitonin, ATP (Sigma-aldrich, St Louis, MO, USA), and assay buffer were added in the blank control wells for reference, and final concentration of Digitonin and ATP was 100 and 50 μM. The sample solution and the cells were incubated for 2.5 min before added agonists capsaicin (Tocris, England) and HCl solution at pH 5 and then

immediately detected. The light emission was recorded during variable times using EnVision2014 Multilabel Reader (PerkinElmer) [17,18].

4.1.2. Analgesic activity

4.1.2.1. Capsaicin test. As previously described, we evaluated analgesic activity in the capsaicin-induced pain model [19]. Twenty microliter of solution of capsaicin (16 μg/20 mL) was injected s.c. under the skin of the dorsal surface of the right hind paw. The mouse was then placed in an individual cage. The amount of time spent licking the injected paw was measured and expressed as the cumulative licking time for 5 min after the capsaicin injection.

4.1.2.2. Abdominal constriction test. Abdominal constriction test was performed as described previously to assess analgesia of pain activated by acid [20]. We placed mice in individual glass cylinders for a 30 min acclimatization period, injected with 0.6% acetic acid (0.1 mL/10 g/mouse i.p.), and immediately placed inside transparent glass cylinders. The number of writhes was recorded for 15 min.

4.1.2.3. Tail-flick test. Tail-flick test was carried out according to previous performance [20]. Briefly, in a water bath maintained at 52 °C, the distal one-third of the mouse tail was immersed. Latency times until a tail-flick response were recorded before and after drug treatment. The antinociception response was presented as percentmaximal possible effect (%MPE) as defined by %MPE = 100% × (drug response time – basal responsetime)/(cut-off time – basal response time). A cut-off time of 12 s was applied to avoid tissue damage.

4.1.3. Effect on body temperature

Mice were intragastric administered with synthesized compounds (30 mg/kg, i.g.), BCTC (30 mg/kg, i.g.), or an equal volume of vehicle. The body temperature of mice was monitored by the electric probe thermometer (MT-1C/F, Ruidien, Shenzhen, China) at 0, 30, 60, 90, and 120 min after dosing. The effect on body temperature was presented as Δ temperature = the temperature at the certain time after dosing – the temperature at 0 min after dosing.

4.1.4. Aqueous solubility

Small volumes of the DMSO solutions of test compounds were diluted to 130 μM by adding second liquid for a disintegration test of Japanese Pharmacopoeia (JP2, pH = 6.8). After incubation at 25 °C for 20 h, precipitates were separated by filtration. The solubility was determined by HPLC analysis of each filtrate.

4.1.5. Pharmacokinetic Study.

The animal studies were performed according to committee approved procedures. Male rats, each weighing 330–380 g (9–10 weeks old), were quarantined for 1 week before use. The animals were surgically implanted with a jugularvein cannula 1 day before treatment and were fasted before treatment. The compound was given to the rats ($n = 3$) as oral (30 mg/kg) dose prepared in a mixture of dosing vehicles. The volume of the dosing solution given was adjusted according to the body weight recorded before the drug was administered. At 0 (immediately before dosing), 1, 2, 4, 6, 8, and 24 h after dosing, a blood sample (~150 mL) was taken from each animal via the jugular-vein cannula and stored in ice (0–4 °C). The processing of the plasma and analysis by high performance liquid chromatography–tandem mass spectrometry (HPLC–MS/MS) was carried out as described. The plasma concentration data were analyzed with a standard noncompartmental method.

4.1.6. Statistical analysis of the data

Statistical analyses were performed using specific software (GRAPHPAD INSTAT version 5.00; GraphPad software, San Diego, CA, USA). Comparisons were analyzed using a one-way analysis of variance (ANOVA) followed by Dunnett's multiple comparison test, unless

otherwise stated. $p < 0.05$ is regarded as statistically significant.

4.2. Chemistry

4.2.1. General

All reagents were purchased from Shanghai Chemical Reagent Company. Column chromatography was carried out on silica gel (200–300 mesh) and monitored by thin layer chromatography performed on GF/UV 254 plates and were visualized by using UV light at 365 and 254 nm. ^1H NMR spectra: BrukerAVANCE III apparatus at 300 MHz, in CDCl_3 unless otherwise indicated; δ in ppm rel. to Me_4Si , J in Hz. ^{13}C NMR spectra: BrukerAVANCE III apparatus at 75 MHz, in CDCl_3 unless otherwise indicated; δ in ppm rel. to Me_4Si . HRMS (high-resolution mass spectra) were taken with a Thermo QE spectrometer, in m/z .

4.2.2. General procedure for the preparation of isoquinolin-5-amine (6)

To a solution of isoquinoline (3.0 g, 23.2 mmol) in 40 mL H_2SO_4 at -15°C was added solid KNO_3 (2.8 g, 27.8 mmol) in four successive equal portions in 30 min. The reaction mixture was warmed to room temperature and stirred for 3 h, then poured into ice-water (100 mL). The pH of the mixture was adjusted to 8–10 with a few drops of ammonia. The precipitated solids were collected by filtration, washed with methyl-tert-butyl ether (100 mL \times 2) and dried to provide **5** (4.0 g, 100% yield) as a yellow solid. To compound **5** (2.5 g, 14.4 mmol) in MeOH (50 mL) was added 10% Pd/C (300 mg), and the mixture was stirred under an atmosphere of hydrogen at room temperature for 3 h. The mixture was filtered and the filtrate was concentrated under vacuum to give the **6** (0.85 g, 41% yield) as a tan solid.

4.2.3. General procedure for the preparation of 10a-w

The solution of 1-(3-dimethylaminopropyl)-3-ethylcarbodiimide hydrochloride (EDCI, 1.78 g, 9.30 mmol) in CH_2Cl_2 (50 mL) with *N*, *N*-dimethylaminopyridine (DMAP, cat) was added dropwise to a stirred solution of Boc-protected *L*-proline **7** (1 g, 4.64 mmol) in CH_2Cl_2 (20 mL) at room temperature. The reaction mixture was stirred at room temperature for 0.5 h. After this period, a solution of substituted phenylamines **8a-w** (4.64 mmol) in CH_2Cl_2 (20 mL) was added dropwise at 0°C . The resulting mixture was then heated to room temperature and stirred, monitored by TLC. Then the reaction mixture was washed with 1 N hydrochloric acid (60 mL \times 2), aqueous brine (60 mL), saturated NaHCO_3 aqueous solution (60 mL \times 2), brine (60 mL), dried over Na_2SO_4 , and concentrated *in vacuo* to provide **9a-w** as yellow solid. The resulting solid of **9a-w** was dissolved in saturated HCl ethyl acetate solution (15 mL) and the reaction mixture was stirred at room temperature, monitored by TLC. Then the resulting solid was filtered and dried under reduced pressure to provide **10a-w** as an HCl salt.

4.2.4. General procedure for the preparation of 3a-w

The solution of **6** (300 mg, 2.08 mmol) in CH_2Cl_2 (20 mL) was added dropwise to a stirred solution of triphosgene (415 mg, 1.39 mmol) in CH_2Cl_2 (20 mL) under nitrogen. Then DMAP (750 mg, 6.15 mmol) was added to the mixture. The reaction mixture was stirred for 30 min, followed by added solution of **10a-w** (2.08 mmol) in CH_2Cl_2 (20 mL) and stirred for an additional 12 h at room temperature. The reaction mixture was monitored by TLC and washed with water to remove DMAP. The organic layer was dried over Na_2SO_4 and concentrated by rotary evaporation to give the red-brown crude product. The residue was purified by flash column chromatography eluting with $\text{CH}_2\text{Cl}_2/\text{CH}_3\text{OH}$ (20:1) to obtain **3a-w**.

4.2.4.1. (R)-*N*¹-(isoquinolin-5-yl)-*N*²-phenylpyrrolidine-1,2-dicarboxamide (3a). Yield 50.5%, red-brown solid, mp = 232.0–234.0 $^\circ\text{C}$; ^1H NMR (DMSO, 300 MHz) δ ppm 10.00 (s, 1H, NH), 9.29 (s, 1H, NH), 8.55 (s, 1H, isoquinoline), 8.46 (d, 1H, $J = 3.0$ Hz, isoquinoline), 7.91–7.86 (m, 2H, isoquinoline), 7.74 (t, 1H, $J = 6.0$ Hz, isoquinoline), 7.63 (t, 3H,

$J = 4.5$ Hz, isoquinoline and Ar-H), 7.29 (t, 2H, $J = 6.0$ Hz, Ar-H), 7.03 (t, 1H, $J = 6.0$ Hz, Ar-H), 4.54 (d, 1H, $J = 6.0$ Hz, CH), 3.81–3.66 (m, 2H, NCH_2), 2.26–2.22 (m, 1H, NCH_2CH_2), 2.02–1.86 (m, 3H, CHCH_2 and NCH_2CH_2); ^{13}C NMR (DMSO, 75 MHz) δ ppm 171.8, 155.2, 152.7, 142.5, 139.6, 135.0, 131.8, 130.9, 129.0, 127.5, 126.4, 124.5, 123.5, 119.6, 117.2, 61.0, 47.2, 30.5, 24.7; HRMS(ESI) Calcd for $\text{C}_{21}\text{H}_{20}\text{N}_4\text{O}_2[\text{M} + \text{H}]^+$ 361.1659, found: 361.1652.

4.2.4.2. (R)-*N*²-(4-bromophenyl)-*N*¹-(isoquinolin-5-yl)pyrrolidine-1,2-dicarboxamide (3b). Yield 80.5%, red-brown solid, mp = 108.3–110.1 $^\circ\text{C}$; ^1H NMR (CDCl_3 , 400 MHz) δ ppm 9.75 (s, 1H, NH), 9.11 (s, 1H, NH), 8.36 (s, 1H, isoquinoline), 7.76 (d, 1H, $J = 9.0$ Hz, isoquinoline), 7.68 (d, 1H, $J = 9.0$ Hz, isoquinoline), 7.50–7.42 (m, 2H, isoquinoline), 7.20 (t, 4H, $J = 9.0$ Hz, Ar-H), 7.01 (s, 1H, isoquinoline), 4.61 (d, 1H, $J = 6.0$ Hz, CH), 3.62–3.32 (m, 2H, NCH_2), 2.32–2.13 (m, 2H, NCH_2CH_2), 2.02–1.86 (m, 2H, CHCH_2); ^{13}C NMR (CDCl_3 , 75 MHz) δ ppm 170.1, 155.9, 152.8, 142.8, 137.3, 132.5, 131.6, 130.9, 129.0, 127.2, 125.6, 125.2, 121.1, 116.3, 114.8, 61.0, 46.9, 27.8, 25.2; HRMS(ESI) Calcd for $\text{C}_{21}\text{H}_{19}\text{BrN}_4\text{O}_2[\text{M} + \text{H}]^+$ 439.0764, found: 439.0761.

4.2.4.3. (R)-*N*²-(3-bromophenyl)-*N*¹-(isoquinolin-5-yl)pyrrolidine-1,2-dicarboxamide (3c). Yield 25.8%, red-brown solid, mp 112.1–114.0 $^\circ\text{C}$; ^1H NMR (CDCl_3 , 300 MHz) δ ppm 9.80 (s, 1H, NH), 9.22 (s, 1H, NH), 8.48 (s, 1H, isoquinoline), 7.90 (d, 1H, $J = 9.0$ Hz, isoquinoline), 7.80 (d, 1H, $J = 3.0$ Hz, isoquinoline), 7.60–7.57 (m, 2H, isoquinoline), 7.47 (d, 1H, $J = 6.0$ Hz, Ar-H), 7.32 (t, 1H, $J = 7.5$ Hz, Ar-H), 7.15 (d, 1H, $J = 9.0$ Hz, Ar-H), 7.07 (t, 1H, $J = 7.5$ Hz, Ar-H), 6.90 (s, 1H, isoquinoline), 4.72 (d, 1H, $J = 6.0$ Hz, CH), 3.80–3.54 (m, 2H, NCH_2), 2.57–2.51 (m, 1H, NCH_2CH_2), 2.36–2.11 (m, 3H, NCH_2CH_2 and CHCH_2); ^{13}C NMR (CDCl_3 , 75 MHz) δ ppm 169.8, 156.1, 152.9, 143.0, 139.5, 132.4, 131.1, 130.2, 130.0, 128.8, 127.2, 126.8, 125.5, 125.2, 124.3, 122.5, 118.1, 61.0, 46.9, 27.7, 25.3; HRMS(ESI) Calcd for $\text{C}_{21}\text{H}_{19}\text{BrN}_4\text{O}_2[\text{M} + \text{H}]^+$ 439.0764, found: 439.0760.

4.2.4.4. (R)-*N*²-(2-bromophenyl)-*N*¹-(isoquinolin-5-yl)pyrrolidine-1,2-dicarboxamide (3d). Yield 18.9%, red-brown solid, mp = 115.9–117.1 $^\circ\text{C}$; ^1H NMR (CDCl_3 , 300 MHz) δ ppm 9.48 (s, 1H, NH), 9.14 (d, 1H, $J = 6.0$ Hz, isoquinoline), 9.06 (s, 1H, NH), 8.43–8.40 (m, 1H, isoquinoline), 8.23 (d, 1H, $J = 3.0$ Hz, isoquinoline), 7.90 (t, 1H, $J = 6.0$ Hz, isoquinoline), 7.70 (t, 1H, $J = 7.5$ Hz, isoquinoline), 7.57 (d, 1H, $J = 3.0$ Hz, Ar-H), 7.52–7.46 (m, 1H, Ar-H), 7.22 (t, 1H, $J = 7.5$ Hz, Ar-H), 6.97 (d, 1H, $J = 3.0$ Hz, isoquinoline), 6.95–6.91 (m, 1H, Ar-H), 4.73 (d, 1H, $J = 6.0$ Hz, CH), 3.73–3.53 (m, 2H, NCH_2), 2.52–2.44 (m, 1H, NCH_2CH_2), 2.18–2.07 (m, 3H, NCH_2CH_2 and CHCH_2); ^{13}C NMR (CDCl_3 , 75 MHz) δ ppm 170.2, 155.8, 152.8, 142.9, 135.8, 133.1, 132.4, 130.9, 129.7, 129.0, 128.2, 127.2, 124.9, 124.6, 122.3, 121.7, 114.4, 61.2, 46.8, 28.6, 25.2; HRMS(ESI) Calcd for $\text{C}_{21}\text{H}_{19}\text{BrN}_4\text{O}_2[\text{M} + \text{H}]^+$ 439.0764, found: 439.0756.

4.2.4.5. (R)-*N*²-(2-chlorophenyl)-*N*¹-(isoquinolin-5-yl)pyrrolidine-1,2-dicarboxamide (3e). Yield 38.9%, red-brown solid, mp = 96.3–98.1 $^\circ\text{C}$; ^1H NMR (CDCl_3 , 300 MHz) δ ppm 9.33 (s, 1H, NH), 9.14 (s, 1H, NH), 8.42 (d, 1H, $J = 6.0$ Hz, isoquinoline), 8.29 (d, 1H, $J = 9.0$ Hz, isoquinoline), 7.83 (d, 1H, $J = 6.0$ Hz, isoquinoline), 7.68 (d, 1H, $J = 9.0$ Hz, isoquinoline), 7.60–7.44 (m, 2H, isoquinoline and Ar-H), 7.35–7.20 (m, 3H, Ar-H), 7.03 (t, 1H, $J = 7.5$ Hz, isoquinoline), 4.70 (d, 1H, $J = 6.0$ Hz, CH), 3.64–3.47 (m, 2H, NCH_2), 2.48–2.46 (m, 1H, NCH_2CH_2), 2.04–1.98 (m, 3H, NCH_2CH_2 and CHCH_2); ^{13}C NMR (CDCl_3 , 75 MHz) δ ppm 170.0, 155.7, 152.7, 142.8, 134.7, 132.5, 130.7, 129.1, 128.9, 127.4, 127.1, 125.6, 124.9, 124.8, 123.5, 122.0, 114.7, 61.2, 46.8, 28.1, 25.1; HRMS (ESI) Calcd for $\text{C}_{22}\text{H}_{19}\text{ClN}_4\text{O}_2[\text{M} + \text{H}]^+$ 395.1269, found: 395.1267.

4.2.4.6. (R)-*N*²-(3-chlorophenyl)-*N*¹-(isoquinolin-5-yl)pyrrolidine-1,2-dicarboxamide (3f). Yield 19.7%, red-brown solid, mp = 209.9–210.4 $^\circ\text{C}$; ^1H NMR (CDCl_3 , 300 MHz) δ ppm 9.88 (s, 1H, NH), 9.16 (s, 1H, NH),

8.43–8.41 (s, 1H, isoquinoline), 7.80 (d, $J = 9.0$ Hz, 1H, isoquinoline), 7.73 (d, $J = 9.0$ Hz, 1H, isoquinoline), 7.61–7.47 (m, 3H, isoquinoline and Ar-H), 7.21 (d, $J = 9.0$ Hz, 1H, Ar-H), 7.07 (t, $J = 9.0$ Hz, 2H, isoquinoline and Ar-H), 6.94 (d, $J = 6.0$ Hz, 2H, Ar-H), 4.67 (d, $J = 6.0$ Hz, 1H, CH), 3.66–3.42 (m, 2H, NCH_2), 2.40 (s, 1H, NCH_2CH_2), 2.19–1.92 (m, 3H, NCH_2CH_2 and $CHCH_2$); ^{13}C NMR ($CDCl_3$, 75 MHz) δ ppm 170.2, 156.0, 152.8, 142.8, 139.4, 134.3, 132.5, 131.0, 129.7, 129.0, 127.2, 125.8, 125.2, 123.9, 119.6, 117.6, 114.9, 61.0, 46.9, 27.7, 25.2; HRMS (ESI) Calcd for $C_{22}H_{19}ClN_4O_2$ [$M+H$] $^+$ 395.1269, found: 395.1267.

4.2.4.7. (R)- N^2 -(4-chlorophenyl)- N^1 -(isoquinolin-5-yl)pyrrolidine-1,2-dicarboxamide (**3g**). Yield 17.9%, red-brown solid, mp = 104.6–105.5 °C; 1H NMR ($CDCl_3$, 300 MHz) δ ppm 9.78(s, 1H, NH), 9.18 (d, 1H, $J = 9.0$ Hz, NH), 8.42 (t, 1H, $J = 7.5$ Hz, isoquinoline), 7.83 (t, 1H, $J = 9.0$ Hz, isoquinoline), 7.74 (t, 1H, $J = 9.0$ Hz, isoquinoline), 7.58 (d, 1H, $J = 6.0$ Hz, isoquinoline), 7.50 (t, 1H, $J = 9.0$ Hz, isoquinoline), 7.42–7.37 (m, 2H, Ar-H), 7.15–7.02 (m, 3H, isoquinoline and Ar-H), 4.69 (d, 1H, $J = 9.0$ Hz, CH), 3.70–3.49 (m, 2H, NCH_2), 2.43 (d, 1H, $J = 15.0$ Hz, NCH_2CH_2), 2.21–1.95 (m, 3H, NCH_2CH_2 and $CHCH_2$); ^{13}C NMR ($CDCl_3$, 75 MHz) δ ppm 170.1, 156.0, 152.8, 142.8, 136.9, 132.6, 131.0, 129.1, 128.7, 127.2, 125.6, 125.1, 120.8, 114.8, 114.7, 61.0, 46.9, 29.6, 25.2; HRMS (ESI) Calcd for $C_{22}H_{19}ClN_4O_2$ [$M+H$] $^+$ 395.1269, found: 395.1266.

4.2.4.8. (R)- N^1 -(isoquinolin-5-yl)- N^2 -(2-methoxyphenyl)pyrrolidine-1,2-dicarboxamide (**3h**). Yield 42.3%, red-brown solid, mp = 105.5–107.1 °C; 1H NMR ($CDCl_3$, 300 MHz) δ ppm 9.17 (s, 1H, NH), 9.12 (s, 1H, NH), 8.43 (d, 1H, $J = 9.0$ Hz, isoquinoline), 8.31 (d, 1H, $J = 6.0$ Hz, isoquinoline), 7.97 (d, 1H, $J = 6.0$ Hz, isoquinoline), 7.71 (d, 1H, $J = 6.0$ Hz, isoquinoline), 7.60–7.49 (m, 2H, isoquinoline and Ar-H), 7.02 (t, 2H, $J = 9.0$ Hz, Ar-H), 6.77 (d, 2H, $J = 6.0$ Hz, Ar-H), 6.93 (d, 1H, $J = 9.0$ Hz, isoquinoline), 6.83 (d, 1H, $J = 9.0$ Hz, Ar-H), 4.70 (s, 1H, CH), 3.77–3.60 (m, 5H, NCH_2 and OCH_3), 2.47–2.37 (m, 2H, NCH_2CH_2), 2.19–2.12 (m, 2H, $CHCH_2$); ^{13}C NMR ($CDCl_3$, 75 MHz) δ ppm 170.0, 155.3, 152.8, 148.3, 142.9, 132.7, 130.4, 129.0, 127.4, 127.2, 124.8, 124.5, 124.1, 120.9, 120.0, 114.4, 110.1, 61.5, 55.7, 46.9, 28.8, 24.9; HRMS (ESI) Calcd for $C_{22}H_{22}N_4O_3$ [$M+H$] $^+$ 391.1765, found: 391.1760.

4.2.4.9. (R)- N^1 -(isoquinolin-5-yl)- N^2 -(4-methoxyphenyl)pyrrolidine-1,2-dicarboxamide (**3i**). Yield 42.3%, red-brown solid, mp = 114.1–116.0 °C; 1H NMR ($CDCl_3$, 300 MHz) δ ppm 9.44 (s, 1H, NH), 9.18 (s, 1H, NH), 8.44 (d, 1H, $J = 3.0$ Hz, isoquinoline), 7.89 (d, 1H, $J = 6.0$ Hz, isoquinoline), 7.75 (d, 1H, $J = 6.0$ Hz, isoquinoline), 7.60–7.51 (m, 2H, isoquinoline), 7.41 (d, 2H, $J = 9.0$ Hz, Ar-H), 7.00 (s, 1H, isoquinoline), 6.77 (d, 2H, $J = 6.0$ Hz, Ar-H), 4.71 (d, 1H, $J = 9.0$ Hz, CH), 3.74 (s, 3H, OCH_3), 3.69–3.53 (m, 2H, NCH_2), 2.50–2.22 (m, 2H, NCH_2CH_2), 2.11–1.95 (m, 2H, $CHCH_2$); ^{13}C NMR ($CDCl_3$, 75 MHz) δ ppm 169.4, 156.1, 152.9, 143.0, 136.8, 132.4, 131.4, 130.7, 129.1, 127.2, 125.2, 125.0, 121.4, 114.5, 114.0, 61.0, 55.4, 46.9, 27.6, 25.3; HRMS (ESI) Calcd for $C_{22}H_{22}N_4O_3$ [$M+H$] $^+$ 391.1765, found: 391.1759.

4.2.4.10. (R)- N^1 -(isoquinolin-5-yl)- N^2 -*p*-tolylpyrrolidine-1,2-dicarboxamide (**3j**). Yield 59.3%, red-brown solid, mp = 205.3–207.1 °C; 1H NMR ($CDCl_3$, 300 MHz) δ ppm 9.62 (s, 1H, NH), 9.04 (s, 1H, NH), 8.30 (d, 1H, $J = 9.0$ Hz, isoquinoline), 7.66 (d, 1H, $J = 6.0$ Hz, isoquinoline), 7.59–7.51 (m, 3H, isoquinoline), 7.39–7.23 (m, 3H, Ar-H), 7.06 (t, 1H, $J = 7.5$ Hz, isoquinoline), 6.82 (d, 1H, $J = 9.0$ Hz, Ar-H), 4.58 (d, 1H, $J = 6.0$ Hz, CH), 3.56–3.41 (m, 2H, NCH_2), 2.30 (d, 1H, $J = 9.0$ Hz, NCH_2CH_2), 2.21 (s, 3H, CH_3), 2.04 (t, 1H, $J = 7.5$ Hz, NCH_2CH_2), 1.88 (s, 2H, $CHCH_2$); ^{13}C NMR ($CDCl_3$, 75 MHz) δ ppm 170.3, 156.1, 152.4, 142.3, 138.6, 138.0, 132.9, 131.2, 128.9, 128.5, 127.1, 126.1, 124.9, 124.8, 120.4, 116.9, 115.5, 61.0, 46.8, 28.2, 24.9, 21.4; HRMS (ESI) Calcd for $C_{22}H_{22}N_4O_2$ [$M+H$] $^+$ 375.1816, found: 375.1812.

4.2.4.11. (R)- N^1 -(isoquinolin-5-yl)- N^2 -*m*-tolylpyrrolidine-1,2-dicarboxamide (**3k**). Yield 85.0%, red-brown solid, mp = 223.6–224.0 °C; 1H NMR ($CDCl_3$, 300 MHz) δ ppm 9.50 (s, 1H, NH), 9.09 (s, 1H, NH), 8.35 (d, 1H, $J = 6.0$ Hz, isoquinoline), 7.72 (d, 1H, $J = 9.0$ Hz, isoquinoline), 7.63 (d, 1H, $J = 9.0$ Hz, isoquinoline), 7.50 (d, 1H, $J = 6.0$ Hz, isoquinoline), 7.40 (t, 1H, $J = 7.5$ Hz, isoquinoline), 7.31 (d, 3H, $J = 6.0$ Hz, Ar-H), 6.98 (d, 2H, $J = 9.0$ Hz, Ar-H and isoquinoline), 4.59 (d, 1H, $J = 9.0$ Hz, CH), 3.57–3.39 (m, 2H, NCH_2), 2.38–2.06 (m, 5H, NCH_2CH_2 and CH_3), 1.90 (t, 2H, $J = 16.5$ Hz, $CHCH_2$); ^{13}C NMR ($CDCl_3$, 75 MHz) δ ppm 169.9, 156.0, 152.6, 142.6, 135.5, 133.6, 132.7, 131.0, 129.3, 129.0, 127.1, 125.7, 124.9, 119.8, 115.0, 60.9, 46.8, 27.8, 25.1, 20.8; HRMS (ESI) Calcd for $C_{22}H_{22}N_4O_2$ [$M+H$] $^+$ 375.1816, found: 375.1812.

4.2.4.12. (R)- N^2 -(3-isopropylphenyl)- N^1 -(isoquinolin-5-yl)pyrrolidine-1,2-dicarboxamide (**3l**). Yield 16.6%, red-brown solid, mp = 98.4–101.1 °C; 1H NMR ($CDCl_3$, 300 MHz) δ ppm 9.53 (s, 1H, NH), 9.15 (s, 1H, NH), 8.41 (d, 1H, $J = 6.0$ Hz, isoquinoline), 7.82 (d, 1H, $J = 6.0$ Hz, isoquinoline), 7.71 (d, 1H, $J = 9.0$ Hz, isoquinoline), 7.57 (d, 1H, $J = 6.0$ Hz, isoquinoline), 7.49 (t, 1H, $J = 9.0$ Hz, isoquinoline), 7.41 (d, 1H, $J = 6.0$ Hz, Ar-H), 7.28 (t, 1H, $J = 7.5$ Hz, Ar-H), 7.16 (t, 1H, $J = 7.5$ Hz, Ar-H), 7.10 (s, 1H, isoquinoline), 6.93 (d, 1H, $J = 9.0$ Hz, Ar-H), 4.68 (d, $J = 6.0$ Hz, 1H, CH), 3.66–3.47 (m, 2H, NCH_2), 2.87–2.78 (m, 1H, NCH_2CH_2), 2.53–2.06 (m, 3H, NCH_2CH_2 and $CHCH_2$), 1.20–1.18 (m, 6H, $C(CH_3)_2$); ^{13}C NMR ($CDCl_3$, 75 MHz) δ ppm 169.8, 156.0, 152.8, 149.8, 142.8, 138.1, 132.6, 130.9, 129.1, 128.7, 127.2, 125.6, 125.0, 122.2, 118.0, 117.3, 114.8, 61.1, 46.9, 34.1, 27.7, 25.2, 23.9; HRMS (ESI) Calcd for $C_{24}H_{26}N_4O_2$ [$M+H$] $^+$ 403.2129, found: 403.2121.

4.2.4.13. (R)- N^2 -(4-*tert*-butylphenyl)- N^1 -(isoquinolin-5-yl)pyrrolidine-1,2-dicarboxamide (**3m**). Yield 23.9%, red-brown solid, mp = 114.0–115.5 °C; 1H NMR ($CDCl_3$, 300 MHz) δ ppm 9.62 (s, 1H, NH), 9.05 (s, 1H, NH), 8.31 (d, $J = 6.0$ Hz, 1H, isoquinoline), 7.60 (d, $J = 3.0$ Hz, 1H, isoquinoline), 7.55 (d, $J = 9.0$ Hz, 1H, isoquinoline), 7.49 (s, 2H, isoquinoline), 7.38–7.29 (m, 3H, isoquinoline and Ar-H), 7.19 (d, $J = 9.0$ Hz, 2H, Ar-H), 4.52 (d, $J = 6.0$ Hz, 1H, CH), 3.47–3.35 (m, 2H, NCH_2), 2.26 (d, $J = 9.0$ Hz, 1H, NCH_2CH_2), 2.00 (t, $J = 7.5$ Hz, 1H, NCH_2CH_2), 1.79 (s, 2H, $CHCH_2$), 1.23 (s, 9H, CH_3); ^{13}C NMR ($CDCl_3$, 75 MHz) δ ppm 170.0, 156.0, 152.6, 146.9, 142.5, 135.6, 132.9, 131.1, 128.9, 127.0, 126.1, 125.9, 125.5, 125.4, 124.9, 119.4, 115.4, 60.9, 46.8, 34.3, 31.3, 31.2, 24.9; HRMS (ESI) Calcd for $C_{25}H_{28}N_4O_2$ [$M+H$] $^+$ 417.2285, found: 417.2280.

4.2.4.14. (R)- N^2 -(4-fluorophenyl)- N^1 -(isoquinolin-5-yl)pyrrolidine-1,2-dicarboxamide (**3n**). Yield 20.6%, red-brown solid, mp = 112.9–114.9 °C; 1H NMR ($CDCl_3$, 300 MHz) δ ppm 9.70 (d, 1H, $J = 3.0$ Hz, NH), 9.08 (d, 1H, $J = 3.0$ Hz, NH), 8.34–8.28 (m, 1H, isoquinoline), 7.72–7.53 (m, 3H, isoquinoline), 7.47–7.33 (m, 4H, isoquinoline and Ar-H), 6.82–6.74 (m, 2H, isoquinoline and Ar-H), 4.60 (d, 1H, $J = 6.0$ Hz, CH), 3.66–3.44 (m, 2H, NCH_2), 2.28–2.91 (m, 4H, NCH_2CH_2 and $CHCH_2$); ^{13}C NMR ($CDCl_3$, 75 MHz) δ ppm 170.5, 160.1, 157.7, 156.0, 152.5, 142.5, 134.3, 132.9, 131.2, 129.0, 127.1, 125.9, 124.9, 121.4, 115.1, 61.0, 45.9, 28.5, 25.0; HRMS (ESI) Calcd for $C_{21}H_{19}FN_4O_2$ [$M+H$] $^+$ 379.1565, found: 379.1561.

4.2.4.15. (R)- N^1 -(isoquinolin-5-yl)- N^2 -(4-methoxy-2-methylphenyl)pyrrolidine-1,2-dicarboxamide (**3o**). Yield 38.7%, red-brown solid, mp = 109.8–111.1 °C; 1H NMR ($CDCl_3$, 300 MHz) δ ppm 9.06 (s, 1H, NH), 8.91 (s, 1H, NH), 8.31 (d, 1H, $J = 6.0$ Hz, isoquinoline), 7.68 (d, 1H, $J = 6.0$ Hz, isoquinoline), 7.61 (d, 1H, $J = 9.0$ Hz, isoquinoline), 7.49 (d, 1H, $J = 6.0$ Hz, isoquinoline), 7.44–7.36 (m, 3H, isoquinoline and Ar-H), 6.55 (d, 2H, $J = 9.0$ Hz, isoquinoline and Ar-H), 4.58 (d, 1H, $J = 9.0$ Hz, CH), 3.66 (s, 3H, OCH_3), 3.49–3.33 (m, 2H, NCH_2), 2.32 (d, 1H, $J = 9.0$ Hz, NCH_2CH_2), 2.99 (d, 4H, $J = 12.0$ Hz, Ar- CH_3 and NCH_2CH_2), 1.93–1.86 (m, 2H, $CHCH_2$); ^{13}C NMR ($CDCl_3$, 75 MHz) δ ppm 170.4, 156.8, 156.0, 152.6, 142.6, 132.9, 132.0, 131.0, 129.0,

128.7, 127.1, 125.7, 124.8, 124.7, 115.7, 115.1, 111.1, 60.7, 55.3, 46.8, 28.0, 25.0, 18.1; HRMS (ESI) Calcd for $C_{23}H_{24}N_4O_3$ $[M+H]^+$ 405.1921, found: 405.1916.

4.2.4.16. (R)-N²-(4-bromo-2-chlorophenyl)-N¹-(isoquinolin-5-yl)pyrrolidine-1,2-dicarboxamide (3p). Yield 23.4%, red-brown solid, mp = 115.5–113.0 °C; ¹H NMR (CDCl₃, 300 MHz) δ ppm 9.46 (s, 1H, NH), 9.17 (s, 1H, NH), 8.45 (d, 1H, *J* = 3.0 Hz, isoquinoline), 8.20 (d, 1H, *J* = 9.0 Hz, isoquinoline), 7.91 (d, 1H, *J* = 6.0 Hz, isoquinoline), 7.73 (d, 1H, *J* = 6.0 Hz, isoquinoline), 7.59 (d, 1H, *J* = 3.0 Hz, isoquinoline), 7.52 (t, 1H, *J* = 6.0 Hz, Ar-H), 7.46 (d, 1H, *J* = 3.0 Hz, Ar-H), 7.33–7.30 (m, 1H, Ar-H), 7.11 (s, 1H, isoquinoline), 4.74 (d, 1H, *J* = 6.0 Hz, CH), 3.72–3.53 (m, 2H, NCH₂), 2.55–2.50 (m, 1H, NCH₂CH₂), 2.15–1.96 (m, 3H, NCH₂CH₂ and CHCH₂); ¹³C NMR (CDCl₃, 75 MHz) δ ppm 170.1, 155.8, 152.9, 143.0, 134.2, 132.4, 131.6, 130.6, 130.4, 129.0, 127.2, 125.3, 124.9, 124.3, 123.0, 116.4, 114.4, 61.2, 46.9, 27.7, 25.2; HRMS (ESI) Calcd for $C_{21}H_{18}BrClN_4O_2$ $[M+H]^+$ 473.0374, found: 473.0371.

4.2.4.17. (R)-N²-(3-chloro-4-methylphenyl)-N¹-(isoquinolin-5-yl)pyrrolidine-1,2-dicarboxamide (3q). Yield 31.2%, red-brown solid, mp = 116.9–118.5 °C; ¹H NMR (CDCl₃, 300 MHz) δ ppm 9.68 (s, 1H, NH), 9.10 (s, 1H, NH), 8.37 (d, 1H, *J* = 6.0 Hz, isoquinoline), 7.75 (d, 1H, *J* = 6.0 Hz, isoquinoline), 7.66 (d, 1H, *J* = 9.0 Hz, isoquinoline), 7.56 (d, 2H, *J* = 3.0 Hz, isoquinoline), 7.44 (t, 1H, *J* = 6.0 Hz, Ar-H), 7.33–7.27 (m, 1H, Ar-H), 7.09 (d, 1H, *J* = 3.0 Hz, isoquinoline), 6.94 (d, 1H, *J* = 6.0 Hz, Ar-H), 4.62 (d, 1H, *J* = 6.0 Hz, CH), 3.66–3.47 (m, 2H, NCH₂), 2.33–2.29 (m, 1H, NCH₂CH₂), 2.22 (s, 3H, CH₃), 2.15–2.11 (m, 1H, NCH₂CH₂), 2.00–1.92 (m, 2H, CHCH₂); ¹³C NMR (CDCl₃, 75 MHz) δ ppm 170.3, 155.9, 152.6, 142.6, 136.9, 134.0, 132.7, 131.2, 131.1, 130.6, 129.0, 127.1, 125.8, 125.0, 120.2, 118.0, 115.1, 61.0, 46.9, 28.2, 25.1, 19.3; HRMS (ESI) Calcd for $C_{22}H_{21}ClN_4O_2$ $[M+H]^+$ 409.1426, found: 409.1421.

4.2.4.18. (R)-N²-(2,6-dimethylphenyl)-N¹-(isoquinolin-5-yl)pyrrolidine-1,2-dicarboxamide (3r). Yield 15.7%, red-brown solid, mp = 109.4–111.6 °C; ¹H NMR (CDCl₃, 300 MHz) δ ppm 9.04 (s, 1H, NH), 8.60 (s, 1H, NH), 8.29 (d, 1H, *J* = 3.0 Hz, isoquinoline), 7.59 (d, 2H, *J* = 6.0 Hz, isoquinoline), 7.48 (d, 2H, *J* = 24.0 Hz, isoquinoline), 7.35 (t, 1H, *J* = 7.5 Hz, Ar-H), 6.94–6.83 (m, 3H, isoquinoline and Ar-H), 4.51 (s, 1H, CH), 3.37–3.24 (m, 2H, NCH₂), 2.10 (s, 1H, NCH₂CH₂), 1.95 (s, 6H, CH₃), 1.81 (s, 3H, NCH₂CH₂ and CHCH₂); ¹³C NMR (CDCl₃, 75 MHz) δ ppm 171.1, 155.9, 152.5, 142.4, 135.1, 133.7, 133.1, 131.1, 128.9, 127.9, 127.0, 125.9, 124.7, 115.4, 60.5, 46.7, 28.7, 24.9, 18.2; HRMS (ESI) Calcd for $C_{23}H_{24}N_4O_2$ $[M+H]^+$ 389.1972, found: 389.1967.

4.2.4.19. (R)-N²-(2,4-dimethylphenyl)-N¹-(isoquinolin-5-yl)pyrrolidine-1,2-dicarboxamide (3s). Yield 21.3%, red-brown solid, mp = 102.2–104.2 °C; ¹H NMR (CDCl₃, 300 MHz) δ ppm 9.20 (d, 1H, *J* = 12.0 Hz, NH), 9.03 (s, 1H, NH), 8.49–8.43 (m, 1H, isoquinoline), 7.98–7.89 (m, 1H, isoquinoline), 7.80–7.68 (m, 2H, isoquinoline), 7.61–7.51 (m, 2H, isoquinoline and Ar-H), 7.06–6.92 (m, 3H, isoquinoline and Ar-H), 4.76 (t, 1H, *J* = 9.0 Hz, CH), 3.73–3.51 (m, 2H, NCH₂), 2.59 (s, 1H, NCH₂CH₂), 2.26 (d, 3H, *J* = 3.0 Hz, CH₃), 2.15 (d, 3H, *J* = 6.0 Hz, CH₃), 2.06–1.97 (m, 3H, NCH₂CH₂ and CHCH₂); ¹³C NMR (CDCl₃, 75 MHz) δ ppm 170.1, 156.0, 152.7, 142.7, 134.5, 133.3, 132.7, 131.0, 130.8, 129.3, 129.0, 127.2, 126.9, 125.5, 124.8, 122.6, 114.8, 60.8, 46.9, 27.8, 25.2, 20.8, 17.8; HRMS (ESI) Calcd for $C_{23}H_{24}N_4O_2$ $[M+H]^+$ 389.1972, found: 389.1968.

4.2.4.20. (R)-N²-(3-chloro-4-methoxyphenyl)-N¹-(isoquinolin-5-yl)pyrrolidine-1,2-dicarboxamide (3t). Yield 42.7%, red-brown solid, mp = 105.3–107.1 °C; ¹H NMR (CDCl₃, 300 MHz) δ ppm 9.63 (s, 1H, NH), 9.19 (s, 1H, NH), 8.47 (d, 1H, *J* = 3.0 Hz, isoquinoline), 7.87 (d, 1H, *J* = 9.0 Hz, isoquinoline), 7.76 (d, 1H, *J* = 9.0 Hz, isoquinoline), 7.61–7.51 (m, 3H, Ar-H and isoquinoline), 7.19 (d, 1H, *J* = 9.0 Hz, Ar-

H), 6.95 (s, 1H, isoquinoline), 6.70 (d, 1H, *J* = 9.0 Hz, Ar-H), 4.68 (d, 1H, *J* = 6.0 Hz, CH), 3.80 (s, 3H, OCH₃), 3.69–3.44 (m, 2H, NCH₂), 2.45–2.21 (m, 2H, NCH₂CH₂), 2.11–1.95 (m, 2H, CHCH₂); ¹³C NMR (CDCl₃, 75 MHz) δ ppm 169.7, 155.9, 152.9, 151.4, 143.0, 132.5, 131.9, 130.8, 129.1, 127.2, 125.4, 125.1, 122.1, 121.9, 119.1, 114.6, 111.9, 60.9, 56.3, 46.9, 27.7, 25.2; HRMS (ESI) Calcd for $C_{22}H_{21}ClN_4O_3$ $[M+H]^+$ 425.1375, found: 425.1370.

4.2.4.21. (R)-N²-(3,4-dichlorophenyl)-N¹-(isoquinolin-5-yl)pyrrolidine-1,2-dicarboxamide (3u). Yield 27.1%, red-brown solid, mp = 105.7–107.6 °C; ¹H NMR (CDCl₃, 300 MHz) δ ppm 9.89 (s, 1H, NH), 9.16 (s, 1H, NH), 8.44 (d, 1H, *J* = 6.0 Hz, isoquinoline), 7.83 (d, 1H, *J* = 9.0 Hz, isoquinoline), 7.75 (d, 1H, *J* = 9.0 Hz, isoquinoline), 7.66 (s, 1H, isoquinoline), 7.60 (d, 1H, *J* = 6.0 Hz, isoquinoline), 7.52 (t, 1H, *J* = 9.0 Hz, Ar-H), 7.13 (s, 2H, Ar-H), 7.05 (s, 1H, isoquinoline), 4.68 (d, 1H, *J* = 9.0 Hz, CH), 3.76–3.52 (m, 2H, NCH₂), 2.51 (s, 1H, NCH₂CH₂), 2.38–1.91 (m, 3H, NCH₂CH₂ and CHCH₂); ¹³C NMR (CDCl₃, 75 MHz) δ ppm 170.4, 155.9, 152.8, 142.8, 137.7, 132.5, 132.3, 131.1, 130.0, 129.1, 127.2, 126.7, 125.8, 125.3, 121.1, 118.8, 114.9, 61.1, 45.9, 28.0, 25.2; HRMS (ESI) Calcd for $C_{21}H_{18}Cl_2N_4O_2$ $[M+H]^+$ 429.0880, found: 429.0879.

4.2.4.22. (R)-N²-(3,5-dimethoxyphenyl)-N¹-(isoquinolin-5-yl)pyrrolidine-1,2-dicarboxamide (3v). Yield 82.7%, red-brown solid, mp = 99.9–101.1 °C; ¹H NMR (CDCl₃, 300 MHz) δ ppm 9.67 (s, 1H, NH), 9.16 (s, 1H, NH), 8.43 (s, 1H, isoquinoline), 7.80 (d, 1H, *J* = 9.0 Hz, isoquinoline), 7.71 (d, 1H, *J* = 6.0 Hz, isoquinoline), 7.55–7.46 (m, 2H, isoquinoline), 7.04 (s, 1H, isoquinoline), 6.75 (d, 2H, *J* = 9.0 Hz, Ar-H), 6.14 (s, 1H, Ar-H), 4.64 (d, 1H, *J* = 6.0 Hz, CH), 3.74–3.60 (m, 7H, 2CH₃ and NCH₂), 3.48 (t, 1H, *J* = 9.0 Hz, NCH₂), 2.45 (s, 1H, NCH₂CH₂), 2.16–1.09 (m, 3H, NCH₂CH₂ and CHCH₂); ¹³C NMR (CDCl₃, 75 MHz) δ ppm 170.1, 160.8, 156.0, 152.8, 142.8, 140.0, 132.6, 130.9, 129.0, 127.1, 125.6, 125.0, 114.9, 97.8, 96.5, 61.1, 55.3, 46.8, 27.7, 25.2; HRMS (ESI) Calcd for $C_{23}H_{24}N_4O_4$ $[M+H]^+$ 421.1870, found: 421.1865.

4.2.4.23. (R)-N¹-(isoquinolin-5-yl)-N²-mesitylpyrrolidine-1,2-dicarboxamide (3w). Yield 21.3%, red-brown solid, mp = 96.8–98.8 °C; ¹H NMR (CDCl₃, 300 MHz) δ ppm 9.14 (d, 1H, *J* = 12.0 Hz, NH), 8.50–8.38 (m, 2H, isoquinoline and NH), 7.88–7.78 (m, 1H, isoquinoline), 7.70 (t, 1H, *J* = 11.5 Hz, isoquinoline), 7.61 (d, 1H, *J* = 3.0 Hz, isoquinoline), 7.53–7.32 (m, 1H, isoquinoline and Ar-H), 6.76 (d, 2H, *J* = 6.0 Hz, isoquinoline and Ar-H), 4.68 (d, 1H, *J* = 12.0 Hz, CH), 3.62–3.47 (m, 2H, NCH₂), 3.13–2.68 (m, 2H, NCH₂CH₂), 2.19 (d, 2H, *J* = 6.0 Hz, CHCH₂), 2.06 (d, 9H, *J* = 9.0 Hz, CH₃); ¹³C NMR (CDCl₃, 75 MHz) δ ppm 171.0, 155.8, 152.7, 142.6, 136.6, 134.9, 133.0, 131.1, 130.9, 129.0, 128.7, 127.1, 125.4, 124.6, 115.0, 60.5, 46.9, 45.8, 29.6, 25.1, 20.8, 18.1; HRMS (ESI) Calcd for $C_{24}H_{26}N_4O_2$ $[M+H]^+$ 403.2129, found: 403.2124.

Acknowledgment

This study was financially supported by the National Natural Science Foundation of China (U1704185) and the Science and Technology Opening and Co-production Project of Henan Province of China (182106000060).

References

- [1] A. Szallasi, D.N. Cortright, C.A. Blum, S.R. Eid, The vanilloid receptor TRPV1: 10 years from channel cloning to antagonist proof-of-concept, *Nat. Rev. Drug Discov.* 6 (2007) 357–372.
- [2] L.M. Broad, S.J. Keding, M.J. Blanco, Recent progress in the development of selective TRPV1 antagonists for pain, *Curr. Top. Med. Chem.* 8 (2008) 1431–1441.
- [3] N. Khairatkar-Joshi, A. Szallasi, TRPV1 antagonists: the challenges for therapeutic targeting, *Trends Mol. Med.* 15 (2009) 14–22.
- [4] J. Luo, E.T. Walters, S.M. Carlton, H. Hu, Targeting pain-evoking transient receptor potential channels for the treatment of pain, *Curr. Neuropharm.* 11 (2013) 652–663.

- [5] T.M. Aghazadeh, P.G. Baraldi, S. Baraldi, S. Gessi, S. Merighi, P.A. Borea, Medicinal chemistry, pharmacology, and clinical implications of TRPV1 receptor antagonists, *Med. Res. Rev.* 37 (2017) 936–983.
- [6] L. De Petrocellis, A.S. Moriello, Modulation of the TRPV1 channel: current clinical trials and recent patents with focus on neurological conditions, *Recent Pat. CNS Drug Discov.* 8 (2013) 180–204.
- [7] G.Y. Wong, N.R. Gavva, Therapeutic potential of vanilloid receptor TRPV1 agonists and antagonists as analgesics: recent advances and setbacks, *Brain Res. Rev.* 60 (2009) 267–277.
- [8] A. Szallasi, G. Appendino, Vanilloid receptor TRPV1 antagonists as the next generation of painkillers. Are we putting the cart before the horse? *J. Med. Chem.* 35 (2004) 2717–2723.
- [9] E.A. Voight, A.R. Gomtsyan, J.F. Daanen, R.J. Perner, R.G. Schmidt, E.K. Bayburt, S. DiDomenico, H.A. McDonald, P.S. Puttfarcken, J. Chen, T.R. Neelands, B.R. Bianchi, P. Han, R.M. Reilly, P.H. Franklin, J.A. Segreti, R.A. Nelson, Z. Su, A.J. King, J.S. Polakowski, S.J. Baker, D.M. Gauvin, L.R. Lewis, J.P. Mikusa, S.K. Joshi, C.R. Faltynek, P.R. Kym, M.E. Kort, Discovery of (R)-1-(7-Chloro-2,2-bis(fluoromethyl)chroman-4-yl)-3-(3-methylisoquinolin-5-yl)urea (A-1165442): a temperature-neutral transient receptor potential vanilloid-1 (TRPV1) antagonist with analgesic efficacy, *J. Med. Chem.* 57 (2014) 7412–7424.
- [10] W.H. Parsons, R.R. Calvo, W. Cheung, Y.K. Lee, S. Patel, J. Liu, M.A. Youngman, S.L. Dax, D. Stone, N. Qin, T. Hutchinson, M.L. Lubin, S.P. Zhang, M. Finley, Y. Liu, M.R. Brandt, C.M. Flores, M.R. Player, Benzod[imidazole transient receptor potential vanilloid 1 antagonists for the treatment of pain: discovery of trans-2-(2-{2-[2-(4-trifluoromethyl-phenyl)-vinyl]-1H-benzimidazol-5-yl}-phenyl)-propan-2-ol (mavatriptan), *J. Med. Chem.* 58 (2015) 3859–3874.
- [11] Y. Lee, S. Hong, M. Cui, P.K. Sharma, J. Lee, S. Choi, Transient receptor potential vanilloid type 1 antagonists: a patent review (2011–2014), *Expert Opin. Ther. Pat.* 25 (2015) 291–318.
- [12] A. Garami, Y.P. Shimansky, E. Pakai, D.L. Oliveira, R.R. Gavva, A.A. Romanovsky, Contributions of different modes of TRPV1 activation to TRPV1 antagonist-induced hyperthermia, *J. Neurosci.* 30 (2010) 1435–1440.
- [13] R.M. Reilly, H.A. McDonald, P.S. Puttfarcken, S.K. Joshi, L. Lewis, M. Pai, P.H. Franklin, J.A. Segreti, T.R. Neelands, P. Han, J. Chen, P.W. Mantyh, J.R. Ghilardi, T.M. Turner, E.A. Voight, J.F. Daanen, R.G. Schmidt, A. Gomtsyan, M.E. Kort, C.R. Faltynek, P.R. Kym, Pharmacology of modality-specific transient receptor potential vanilloid-1 antagonists that do not alter body temperature, *J. Pharmacol. Exp. Ther.* 342 (2012) 416–428.
- [14] A. Gomtsyan, E.K. Bayburt, R.G. Schmidt, G.Z. Zheng, R.J. Perner, S. DiDomenico, J.R. Koenig, S. Turner, T. Jinkerson, I. Drizin, S.M. Hannick, B.S. Macri, H.A. McDonald, P. Honore, C.T. Wismer, K.C. Marsh, J. Wetter, K.D. Stewart, T. Oie, M.F. Jarvis, C.S. Surowy, C.R. Faltynek, C.-H. Lee, Novel transient receptor potential vanilloid 1 receptor antagonists for the treatment of pain: structure-activity relationships for ureas with quinoline, isoquinoline, quinazoline, phthalazine, quinoxaline, and cinnoline moieties, *J. Med. Chem.* 48 (2005) 744–752.
- [15] R. El Kouhen, C.S. Surowy, B.R. Bianchi, T.R. Neelands, H.A. McDonald, W. Niforatos, A. Gomtsyan, C.-H. Lee, P. Honore, J.P. Sullivan, M.F. Jarvis, C.R. Faltynek, A-425619 [1-isoquinolin-5-yl-3-(4-trifluoromethyl-benzyl)-urea], a novel and selective transient receptor potential type V1 receptor antagonist, blocks channel activation by vanilloids, heat, and acid, *J. Pharmacol. Exp. Ther.* 314 (2005) 400–409.
- [16] M.E. Kort, P.R. Kym, TRPV1 antagonists: clinical setbacks and prospects for future development, *Prog. Med. Chem.* 51 (2012) 57–70.
- [17] E. Le Poul, S. Hisada, Y. Mizuguchi, V.J. Dupriez, E. Burgeon, M. Detheux, Adaptation of aequorin functional assay to high throughput screening, *J. BiomolScreen.* 7 (2002) 57.
- [18] S.G. Lehto, R. Tamir, H. Deng, L. Kliensky, R. Kuang, A. Le, D. Lee, J.C. Louis, E. Magal, B.H. Manning, J. Rubino, S. Surapaneni, N. Tamayo, T. Wang, J. Wang, J. Wang, W. Wang, B. Youngblood, M. Zhang, D. Zhu, M.H. Norman, N.R. Gavva, Antihyperalgesic effects of (R, E)-N-(2-hydroxy-2,3-dihydro-1H-inden-4-yl)-3-(2-(piperidin-1-yl)-4-(trifluoromethyl)phenyl)-acrylamide (AMG8562), a novel transient receptor potential vanilloid type 1 modulator that does not cause hyperthermia in rats, *J. Pharmacol. Exp. Ther.* 326 (2008) 218–229.
- [19] T. Sakurada, A. Sugiyama, C. Sakurada, K. Tan-No, A. Yonezawa, S. Sakurada, K. Katsura, Effect of spinal nitric oxide inhibition on capsaicin-induced nociceptive response, *Life. Sci.* 59 (1996) 921–930.
- [20] L. Tang, Y. Chen, Z. Chen, P.M. Blumberg, A.P. Kozikowski, Z.J. Wang, Antinociceptive pharmacology of N-(4-chlorobenzyl)-N'-(4-hydroxy-3-iodo-5-methoxybenzyl) thiourea, a high-affinity competitive antagonist of the transient receptor potential vanilloid 1 receptor, *J. Pharmacol. Exp. Ther.* 321 (2007) 791–798.